Effect of spacer layer thickness on magnetic interactions in self-assembled single domain iron nanoparticles

Nichole B. Herndon, Sang Ho Oh, Jeremiah T. Abiade, Devdas Pai, Jag Sankar, Stephen J. Pennycook, and Dhananjay Kumar

Articles you may be interested in

Effect of spacer layer thickness on magnetic interactions in self-assembled single domain iron nanoparticles

Nichole B. Herndon,[1] Sang Ho Oh,[1,2] Jeremiah T. Abiade,[3] Devdas Pai,[1] Jag Sankar,[1]
Stephen J. Pennycook,[2] and Dhananjay Kumar[1,2,a]

[1]*Center for Advanced Materials and Smart Structures, Department of Mechanical and Chemical
Engineering, North Carolina Agricultural and Technical State University, North Carolina 27411, USA*
[2]*Materials Science and Technology Division, Oak Ridge National Laboratory, Oak Ridge, Tennesse 37831,
USA*
[3]*Department of Materials Science and Engineering and Department of Mechanical Engineering, Virginia
Polytechnic Institute and State University, Blacksburg, Virginia 24061, USA*

The magnetic characteristics of iron nanoparticles embedded in an alumina thin film matrix have
been studied as a function of spacer layer thickness. Alumina as well as iron nanoparticles were
deposited in a multilayered geometry using sequential pulsed laser deposition. The role of spacer
layer thickness was investigated by making layered thin film composites with three different spacer
layer thicknesses (6, 12, and 18 nm) with fixed iron particle size of ~13 nm. *Intralayer* magnetic
interactions being the same in each sample, the variation in coercivity and saturation magnetization
is attributed to thickness dependent *interlayer* magnetic interactions of three types: exchange, strong
dipolar, and weak dipolar. A thin film composite multilayer structure offers a continuously tunable
strength of *interparticle* dipole-dipole interaction and is thus well suited for studies of the influence
of interaction on the magnetic properties of small magnetic particle systems. © *2008 American
Institute of Physics.* [DOI: 10.1063/1.2833309]

Materials consisting of self-assembled nanosized magnetic particles embedded in a host matrix have received considerable attention since they offer the potential to satisfy the critical needs of data storage devices.[1–3] Magnetic nanoparticles assembled in an insulating matrix can also provide great insight into the physics of magnetic interactions.[4] Assemblies of small magnetic particles have been synthesized predominantly using chemical processes where *interparticle* separation is manipulated by controlling the volume fraction of particulate systems in host matrices.[5–8] Using an exclusive chemical process, however, it is a challenge to fabricate nanoparticle thin film composite in a multilayered geometry which is important for the device applications of nanocomposites.[9–12] In this paper, we report our investigation on the role of spacer layer thickness on magnetic interaction and resulting magnetic properties of nanoparticles assembled in a three dimensional structure using a pulsed laser deposition (PLD) method.

A multitarget PLD system was used where iron and alumina targets were alternately ablated. The details of PLD process parameters are reported in our previous publications.[13,14] The thickness of first Al_2O_3 layer, which serves as barrier layer was 75 nm, is significantly larger than the thicknesses of Al_2O_3 in subsequent layers, where it acts as spacer layer. While the size of Fe nanocrystals was kept fixed in all the samples, the thickness of Al_2O_3 layer was varied from sample to sample by varying the number of laser

pulses impinging on the A_2O_3 target. The numbers of alternating layers (Fe and Al_2O_3) were five.

The size of Fe particles, the exact thickness of the spacer layer, and interparticle separation were investigated by cross-sectional scanning transmission electron microscopy (STEM). Shown in Fig. 1(a) is the STEM image of five layered Fe–Al_2O_3 sample prepared using 1500 pulses of laser on Fe target and 166 pulses on Al_2O_3 target. The average Fe particle size is ~13 ± 5 nm, the average *intralayer* particle separation is ~3 nm, and the interparticle separation is ~6 nm. Though the majority of particles in one layer are physically separated from the particles in layers above or below it, in some regions, the interparticles are in direct contacts with each other. A similar STEM image of another sample prepared using 500 laser pulses on Al_2O_3 target is shown in Fig. 1(b). The number of laser pulses on Fe target was fixed as in the previous sample, i.e., 1500. Clearly, the spacer layer thickness has increased (~18 nm) and the particles in one layer are well separated from the particles in the other layers. The particle size as well as intralayer particle separation are almost the same as the last sample. As seen in the two insets in Fig. 1, the interface between Fe nanoparticle and the surrounding Al_2O_3 matrix in both samples is clean and sharp, indicating the presence of pure metallic Fe at the surface. Looking at the absolute value of the heat of formation (ΔH_f) for the most stable iron oxide (-39.2 kcal/g atom), one might speculate the formation of an oxide layer on the Fe particle surface more when the matrix surrounding the nanoparticles is an oxide.[15,16] However, the ΔH_f for iron oxide is almost twice the ΔH_f of aluminum oxide (-80.2 kcal/g atom).[15,16] The more negative the value of the

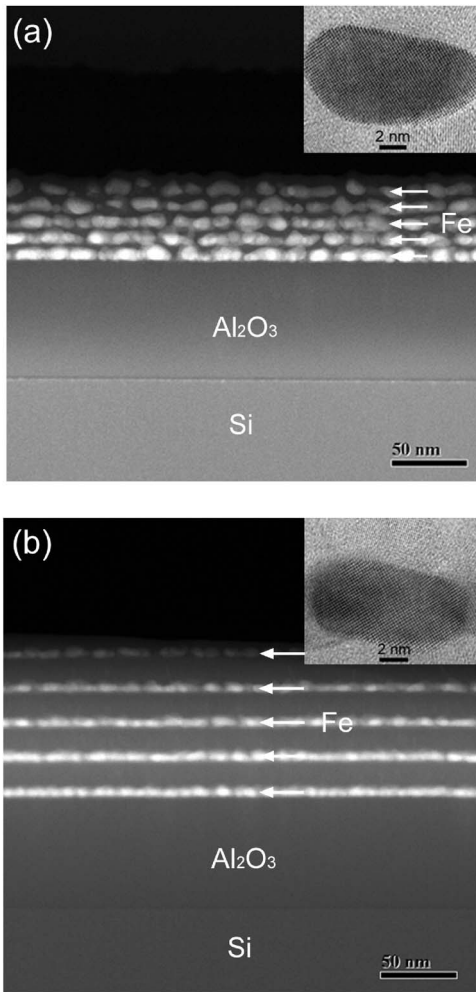a)Author to whom correspondence should be addressed. Electronic mail:
dkumar@ncat.edu.

FIG. 1. STEM high angle annular dark-field images of (a) Fe–Al$_2$O$_3$ multilayer with 6 nm thick Al$_2$O$_3$ spacer layers and (b) Fe–Al$_2$O$_3$ multilayer with 18 nm thick Al$_2$O$_3$ spacer layers. The insets are STEM bright-field images of single isolated Fe particles embedded in Al$_2$O$_3$ spacer layers.

ΔH_f, the more strong the element bonds to oxygen. Besides, all the sample fabrications are carried out in high vacuum condition ($\sim 10^{-7}$ torr). Our previous atomic level structural characterization study by means of STEM and electron energy loss spectroscopy on nanoparticles of Ni [which has a similar ΔH_f for its stable oxide (-28.8 kcal/g atom) embedded in A$_2$O$_3$ thin film matrix using the PLD and similar deposition conditions] had proved the absence of any oxide layer on the Ni nanoparticle surface.[14] Thus, based on the heat of formation data and the structural characterization information of Ni–Al$_2$O$_3$,[14] it is reasonable to assume that the Fe nanoparticles in Al$_2$O$_3$ matrix have very high likelihood to be free from any appreciable oxide dead layer in the present study.

The magnetic properties of Fe–Al$_2$O$_3$ systems were measured using a vibrating sample magnetometer interfaced with a physical property measurement system. Figure 2 shows the magnetic moment versus field loops at 10 K for Fe–Al$_2$O$_3$ samples having three different spacer layer thicknesses. The magnetic moment versus field loops were also recorded at several other temperatures between 10 and 300 K for samples with different spacer layer thicknesses. The re-
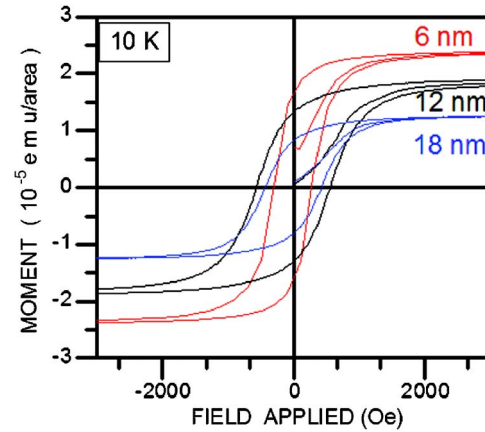

FIG. 2. (Color online) Magnetic moment vs field applied loops at 10 K for samples with 6, 12, and 18 nm thick spacer layer Al$_2$O$_3$.

sults are plotted in Fig. 3 in the form of H_c vs $\sqrt{T}$. The coercivity values of the sample with 12 nm thick Al$_2$O$_3$ spacer layer are higher than that of the other two samples at all the temperatures. In an assembly of single domain magnetic particles, the magnetic field (H_c) required to reverse their magnetization is given by the equation,

$$H_c = 2K/M_s[1 - (T/T_B)^{1/2}], \tag{1}$$

where T_B ($=KV/25k_B$ for uniaxial anisotropy) is called the blocking temperature where the metastable hysteretic response is lost for a particular observation time. Here, K is the anisotropy constant of the particle material, V is the volume of the particle, and M_s is the saturation magnetization. KV is thus the anisotropy energy barrier for the reversal of magnetization. As shown in Fig. 3, the iron particles follow this relationship closely in all three samples with different spacer layer thicknesses. This trend suggests the presence of assemblies of noninteracting magnetic particles with uniaxial anisotropy on the basis of Néel's concept of superparamagnetism. However, in a dense systems, such as in the present study (volume fraction of nanoparticles=0.43 for 6 nm Al$_2$O$_3$, 0.33 for 12 nm Al$_2$O$_3$, and 0.26 for 18 nm Al$_2$O$_3$ spacer layer samples), the interparticle interaction is known to modify the magnetic behavior of the assembly.[7,17,18] The values of T_B obtained from the fitting of the H_c (T) data to
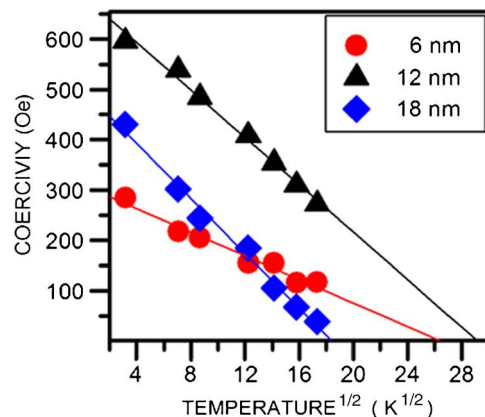

FIG. 3. (Color online) Coercivity as a function of temperature with the data fitted to equation $H_c = 2K/M_s[1 - (T/T_B)^{1/2}]$.

Eq. (1) are 690, 846, and 336 K, respectively, for samples with 6, 12, and 18 nm thick Al_2O_3 spacer layers. The variation of T_B for samples with the same particle size in a matrix with different spacer layer thicknesses can be explained using the concept of magnetic interactions in dispersed magnetic nanoparticle assemblies.[17–20]

Two types of interaction mechanisms—dipolar and exchange—can operate between nanoparticles depending on the interparticle distances and agglomeration. Since the matrix (Al_2O_3) in the present study is insulating and nonmagnetic, the interaction among Fe nanoparticles is expected to be predominantly dipolar. However, if the spacer layer is very thin, it may not be able to separate the magnetic particles completely in one layer from magnetic particles in the next layer and so on over the entire macroscopic sample in a uniform fashion. As seen in Fig. 1(a), some of the Fe nanoparticles in one layer are *indeed* in direct contact with Fe particles in neighboring layers. When the magnetic particles are in contact with each other, the exchange type of interparticle interaction dominates where atomic spins within a particle are coupled. When the Al_2O_3 spacer layer thickness is increased to 12 nm, the possibility of *interlayer* Fe particle contacts is greatly diminished which, in turn, promotes the dipolar interaction mechanism. The strength of dipolar interaction is determined by two parameters, namely, the average distance between the particles and their size.[20,21] Since the particle size and interparticle separation in a given layer are fixed, it is reasonable to assume that magnetic interaction in the intralayer is the same in all the three samples. Therefore, an increase in T_B of 12 nm Al_2O_3 spacer layer sample by nearly 20% with respect to that of 10 nm Al_2O_3 spacer layer sample can be attributed to change in interlayer interaction mechanism to dipolar type from exchange type. An increase in T_B by a factor of up to 2 has been observed for magnetic nanoparticle dispersions with the same particle size but with a different volume fraction, which, in turn, affects the interactions among magnetic particles.[17–20] The decrease in T_B and H_c with further increase in spacer layer thickness (i.e., at 18 nm) can be explained by the decrease in the strength of interparticle dipolar strength. The dipolar interaction can be weak, moderate, or strong, depending on the level of volume fraction.[17–19]

In summary, we have fabricated multilayered samples with fixed Fe nanoparticle size and variable spacer layer thickness using a physical vapor deposition based PLD process. The variation of coercivity values as a function of spacer layers indicates the existence of an optimum thickness of a spacer layer to realize strong magnetic dipolar interaction and, hence, to realize high values of coercivity at higher temperatures in a given system. The ability to change interlayer particle interaction without changing intralayer particle interaction by means of spacer layer thickness variation can provide a convenience means to study the physics of interactions among magnetic nanoparticles.

[1]S. Sun, C. B. Murray, D. Weller, L. Folks, and A. Moser, Science **287**, 1989 (2000).
[2]C. L. Chien, Annu. Rev. Mater. Sci. **25**, 129 (1995).
[3]O. Santini, D. H. Mosca, W. H. Schreiner, R. Marangoni, J. L. Guimarães, F. Wypych, and A. J. A. de Oliveira, J. Phys. D **36**, 428 (2003).
[4]J. S. Moodera, L. R. Kindler, T. M. Wong, and R. Meservey, Phys. Rev. Lett. **74**, 3273 (1995).
[5]V. Russier, C. Petit, J. Legrand, and M. P. Pileni, Phys. Rev. B **62**, 3910 (2000).
[6]Y. Lalatonne, L. Motte, V. Russier, A. T. Ngo, P. Bonville, and M. P. Pileni, J. Phys. Chem. B **108**, 1848 (2004).
[7]D. Farrel, Y. Cheng, R. W. Mccallum, M. Achan, and S. A. Majetich, J. Phys. Chem. B **109**, 13409 (2005).
[8]X. M. Lin, C. M. Sorensen, K. J. Klabunde, and G. C. Hadjipanayis, Langmuir **14**, 7140 (1998).
[9]C. P. Collier, J. O. Jeppesen, Y. Luo, J. Perkins, E. W. Wong, J. R. Heath, and J. F. Stoddart, J. Am. Chem. Soc. **123**, 12632 (2001).
[10]T. Cui, F. Hua, and Y. Lvov, IEEE Trans. Electron Devices **51**, 503 (2004).
[11]C. Joachim, J. K. Gimzewski, and A. Aviram, Nature (London) **408**, 541 (2000).
[12]M. Ollsen, B. Persson, and L. Salford, Magn. Reson. Imaging **4**, 437 (1986).
[13]D. Kumar, J. Narayan, A. V. Kvit, A. K. Sharma, and J. Sankar, J. Magn. Magn. Mater. **232**, 161 (2001).
[14]D. Kumar, A. Lupini, S. J. Pennycook, J. Narayan, and G. Duscher, Appl. Phys. Lett. **81**, 4204 (2002).
[15]R. K. Singh and D. Kumar, Mater. Sci. Eng., R. **22**, 113 (1998).
[16]R. S. Williams and S. Chaudhury, in *Chemistry of High Temperature Superconductors II*, edited by D. L. Nelson and T. F. George (American Chemical Society, Los Angeles, CA, 1988), p. 291.
[17]D. Kechrakos and K. N. Trohidou, Phys. Rev. B **58**, 12169 (1998).
[18]J. L. Dorman, L. Bessais, and D. Fiorani, J. Phys. C **21**, 2015 (1988).
[19]S. Gangopadhyay, G. C. Hadjipanayis, C. M. Sorenson, and K. J. Klabunde, IEEE Trans. Magn. **29**, 2619 (1993).
[20]R. W. Chantrell, M. El-Hilo, and K. O'Grady, IEEE Trans. Magn. **27**, 3570 (1991).
[21]A. Ceylan, C. C. Baker, S. K. Hasanain, and S. Ismat Shah, Phys. Rev. B **72**, 134411 (2005).